Egypt. J. Chem. **Vol. 66**, No. 10 pp. 125 - 131 (2023)

Egyptian Journal of Chemistry

http://ejchem.journals.ekb.eg/

Performance of Imported Granulated Blast-Furnace Slag (IGBFS) Rich Cement Against Fire Resistance

Hazem I. Bendary,[a]Mohamed Heikal,[b] and Mohamed A. Ali[c]*

[a]*Chemical Engineering Department, Higher Institute of Engineering, , El-Shorouk Academy, Shorouk City, Cairo, Egypt*

[b]*Chemistry Department, Faculty of Science, Benha University, Benha, Egypt*

[c]*School of Biotechnology, Badr University in Cairo (BUC), Badr City, Cairo, 11829, Egypt*

Abstract

The effect of firing temperature on the properties of pozzolanic cement was assessed. A set of specimens were prepared by mixing different mass ratios (40%, 50%, 60% and 70%) of imported granulated blast furnace slag, (IGBFS) with Ordinary Portland cement, (OPC). Different dosages of GBFS were investigated for weight loss, bulk density, total porosity, and mechanical compressive strength. The results show that the weight loss as well as the porosity for all mix proportions increases in the same trend with firing temperature. Quite in contrast, the bulk density and compressive strength gradually decrease with firing temperature. Finally, recrystallization, phase change, distortion, and other hydration products were investigated using XRD. The research also suggested using the specimen with more slag as a fire-resistant bonding material, which has significant environmental and financial benefits.

Keywords: Fire resistance; Weight loss; Compressive strength; and pozzolanic cement

1. Introduction

Fires are regular catastrophes that pose a major threat to both human life and property.

After a fire, strengthening and restoring the bearing capacity and employing the function of the building are based on performance analysis and evaluation of the burned building's construction. It is unquestionably crucial to assess how typical structural materials behave after being exposed to high temperatures. Under conditions of high temperatures, concrete experiences severe and complicated physical and chemical changes that impair performance and even eliminate its load-bearing capacity. Weight loss, colour change, increased porosity, cracking, and bursting is some of the physical modifications that high temperatures can cause to concrete [1–4].

Many organizations and countries have stated their intentions to become carbon neutral by 2050 in response to the urgent need to address global warming and climate change [5]. Carbon capture and storage technologies are considered promising means of achieving this aim [6], particularly for cementitious materials, which may safely and permanently capture and store CO_2 [7–10]. Consequently, tremendous effort is made to lower cement use. It also involves the use of alternative binders and supplemental cementitious materials like fly ash, GGBFS, etc.

Replacing OPC partially with silica fume improves the physical, mechanical, and microstructural characteristics of concrete when exposed to high temperatures [11, 12] When subjected to high temperatures followed by high humidity or soaking, Portland cement with 20 to 30 weight percent fly ash more stable and maintains its dimensions during exposure to fire [13].

*Corresponding author e-mail: Mohamed.ahmed_ali@buc.edu.eg; (Mohamed A. Ali).
EJCHEM use only: Received date 11 November 2022; revised date 08 January 2023; accepted date 30 January 2023
DOI: 10.21608/EJCHEM.2023.173658.7179

On the other hand, on replacing (OPC) with 15 % meta kaolin and 5 % silica fume, the resistance of all prepared samples against thermal shock was enhanced by nearly ten times[14]. Burning up to 800^{o}C increases mechanical strength, porosity, and fire resistance while decreasing free lime content and bulk density for pozzolanic cement paste prepared with 20 wt% Homra as compared to OPC [15].

Recent research used the mineralogical analysis of cement paste to find that carbonation has an appositive effect on the resistance of cement pastes to high temperatures up to 500 ºC but this property is lost at 600 ºC [16]. Experimental work showed that using untreated RHA up to 10% in cement mortar doesn't affect the mechanical strength which is reduced gradually with high doses till 30% at which compressive strength starts to increase. For all doses, the resistance against heat was positively affected except those have 20% RHA [17].

Ground granulated blast furnace slag (IGBFS) is a glassy, granular by-product formed in the steel manufacturing process as a result of quenching molten iron from a blast furnace in water or steam, it is rich in amorphous calcium, silica and alumina, which makes it a material with good bonding properties employed in the construction industry [18, 19]. 65% of the highly abundant slag (530 million tons/year) is used as cemenitious material in the construction sector [20].

The utilization of IGBFS in the construction industry improves durability and helps to prevent early-age thermal cracking, it is also cost-effective [21]. This work aims to produce a good fire-resistant blend using iron slag by-product in high proportions as a partial substitute for OPC in cement pastes which will have a positive environmental and economic impact.

2. Experimental Work

2.1. Starting materials and their characterization

(OPC) utilized in this experimental work came from Suez Cement Company, while (IGBFS) was purchased and provided by (Kokan Mining Co. LTD, Japan). A laboratory-size, 5 kg steel ball mill is used to grind the slag into a fine powder. Using the Blaine air-permeability equipment with the ASTM technique [22], the specific surface area shown in table (1) was calculated. Table (2) displayed the results of chemical analysis for utilized materials.

Table (1)
The specific surface areas of starting materials

Starting Materials	IGBFS	OPC
Specific Surface Area (cm^2/g)	4300	3050

The (OPC) major phase content is as follows:

C_3S = 52.0%, C_2S = 19.20%, C_3A = 8.80 and C_4AF = 11.08%.

The diffractogram of the unreacted slag shows a predominantly amorphous material as shown in Figure (1). There is also a broad feature 'amorphous hump' between 20 and 38 2θ^{o} attributed to the amorphous glassy component. An amorphous glassy phase exceeds 90% by wt. (IGBFS) was investigated mineralogically by X–Ray diffraction analysis (XRD) in a previous work [18, 23, 24].

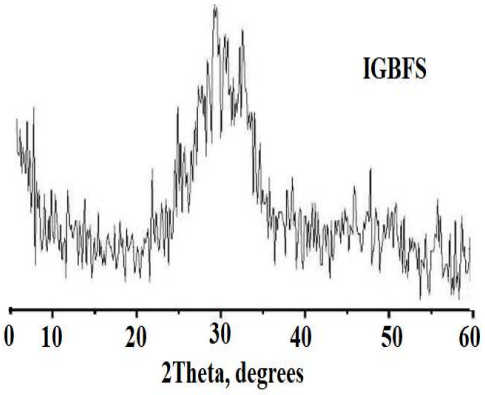

Figure (1): XRD pattern of Imported GBFS

Table (2)
Chemical constituents of beginning materials (wt. %)

Item	SiO_2	Al_2O_3	Fe_2O_3	CaO	MgO	Na_2O	K_2O	BaO	SO_3	S^{--}	L.O.I
IGBFS	37.48	12.86	0.40	37.70	2.45	1.84	0.93	5.31	0.01	0.75	0.0
OPC	20.51	5.07	4.39	62.21	2.00	0.23	0.29	0.0	2.25	0.0	2.40

2.2. Preparation of Anhydrous Pozzolanic Cements

The GBFS was crushed using a jaw crusher and then finely milled using a laboratory steel ball mill with a (5 kg) capacity. Table (3) displays the weight percentage of the dry components of OPC, IGBFS blend that was mechanically combined for (1hr) in porcelain ball mill to achieve total homogeneity and then stored in airtight containers until the fabrication of cement paste.

Mixing of Pozzolanic Cement Pastes:

The standard water of consistency is used to prepare all specimens. Table (3) illustrates the used water of consistency (Wt. %) as determined by [25] for different blended cement pastes.

Table (3)
The water of consistency (Wt. %) for different batches

Mix No	OPC	Slag	Water of consistency %
A1	30	70	26.50
A2	40	60	26.85
A3	50	50	27.10
A4	60	40	27.30

2.3. Moulding

One-inch cubic moulds were employed to determine the compressive strength.

2.4. Curing

The casted cubes were treated for the first 24 hrs. In a 100% humid chamber at 25 °C. The moulds were removed and then, placed in fresh water to cure for 28 days.

2.5. Firing

At 105°C, cured specimens were dried for (24 hr.) to eliminate humidity, then thermally treated with 10°C/min of heating, The specimens were held at the specified temperatures (105, 250, 450, 600 and 800°C) two hours to attain the thermal steady state, after which they were brought to room temperature, [26]. The specimens could now be tested.

3. Results and discussion

3.1. The Weight loss

The following mathematical equation was adapted to illustrate the cement pastes reaction to fire exposure:

$$\text{Ignition Loss, \%} = \frac{wi-wf}{wf} \times 100 \quad (1)$$

W_i is the weight before ignition, and
W_f is the weight after ignition.

The weight loss of different specimens (A1, A2, A3 and A4) with respect to treatment temperatures up to 800°C illustrated visually in Figure (2). Due to the disintegration of various hydration products, as was acknowledged [27, 28], the weight loss gradually increases with increasing temperature up to 800°C.

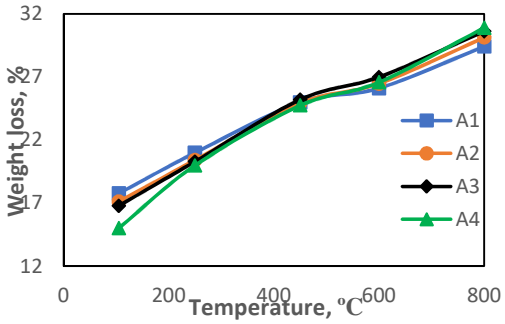

Figure (2): Loss of weight when slag-cement pastes are heated to 800°C

It has been demonstrated that up to 600°C, A1, A2, and A3 lose weight more quickly than A4. The weight loss of A4 is greater than that of any other cement pastes at a higher temperature, 800°C. It's possible that A4's weight loss at 800 °C increased because there were more $CaCO_3$ present thanks to the carbonation of CH into $CaCO_3$. These pastes provide higher free lime content that is frequently carbonated.

3.2. Bulk density measurements:

To calculate the saturated weight of the samples, four chips from each mix composition were collected, burned at the appropriate temperature, and then submerged in kerosene (0.8 g/cm^3) for a full day. The samples were then reweighed while suspended in kerosene, and their dried weight was calculated after 24 hours of drying at 105 ºC in the air. The following equation was used to evaluate the bulk density:

$$\text{Bulk density (dp)} = \frac{SaturatedWeight}{SaturatedWeight - SuspendedWeight} \text{g/cm}^3 \quad (2)$$

The evaluated density of treated pozzolanic samples with varied dosages of IGBFS is plotted with the treatment temperature up to 800°C in Figure (3). The three phases involved in changing the bulk density of variously treated cement pastes are as follows. In general, up to 250°C, the temperature affects apparent density negatively (first step) due to the elimination of free or adsorbed as well as combined water contents of CSH or CAH. The density is nearly the same in the second stage, which occurs between 250 and 400 °C. All pozzolanic cement pastes see an increase in density during the third step (from 400–800°C) due to the decomposition of $Ca(OH)_2$ to CaO which reacts to amorphous aluminosilicate leads to denser structure, A4 cement paste that is rich in OPC gained the highest apparent density. This is mostly explained by the hydration yield growth, which results in a denser structure. This forms also some ceramic minerals with high bulk density, due to the reaction of CH with pozzolanic material (IGBFS).

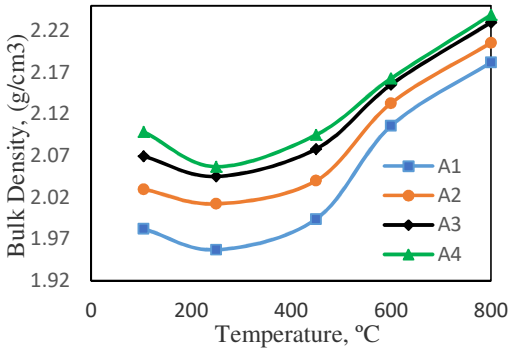

Figure (3): Bulk density of various doses versus treatment temperature

3.3. Total porosity (ε):

Using the results of weight calculations obtained previously, it is possible to find the total porosity as follows:

$$\varepsilon = \frac{SaturatedWeight - DriedWeight}{SaturatedWeight - SuspendedWeight} \times 100 \quad (3)$$

The porosity of heat-treated samples for different doses of (IGBFS) at the aforementioned temperatures is graphically plotted in Figure (4). The change in porosity goes through two main steps in the same trend. Initially, (up to 250 °C), total porosity decreases with temperature as it coincides with an increase in cement hydration products that fill the pores in the presence of a pozzolanic reaction. The second step, which starts at 450 and ends at 800 °C, where an increase in porosity is observed, is explained by the dehydroxylation of free CH and the decomposition of ($CaCO_3$) to (CaO), which is responsible for the appearance of micro cracks involved with a significant coarsening of the pore size distribution in the specimens [29, 30]. A1 (rich in slag) achieved the lowest porosity values than other cement pastes, starting from 105 to 450 ºC where the pozzolanic activity increases with temperature increasing. On the other hand, A4 (poor in slag) gained the lowest porosity values at the temperature range (450-800 ºC) where (IGBFS)% content was responsible for slowing the rate of hydration of slag cement pastes.

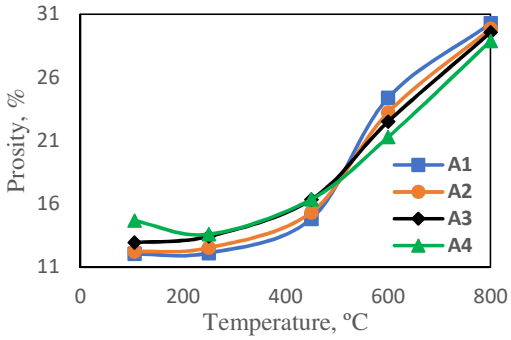

Figure (4): The effect of thermal treatment temperature on porosity

3.4. Compressive strength determination:

Four cubes were used to determine the mechanical strength of the previously prepared samples [31].

Figure (5) illustrates the effect of temperature which ranged from 105 to 800 °C on the compressive strength of thermally treated specimens with different (IGBFS) doses. The compressive strength increases as the treated temperature rise to 250 °C before declining up to 800 °C. The increase in cement paste hydration products and the pozzolanic reaction of (IGBFS) with CH to produce larger amounts of CSH with a low Ca/Si ratio and high strength are both responsible for the increase in compressive strength up to 250 °C [32]. This is also because of the internal self-autoclaving effect, which results from the accumulation of steam created by the removal of capillary, adsorbed, and mixed water at high temperatures. This steam pressure increase speeds up the hydration of cement pastes to form dense structures [33]. Compressive strength decreases significantly at 800 °C as a result of severe deterioration of CSH gel and water layer expansion in

cement pastes [34]. Additionally, because the pore size distribution has become more coarse, the porosity has increased. It may be inferred that the 70 wt% (IGBFS) pozzolanic cement pastes are more heat resistant than the other pozzolanic cement pastes at all temperatures. This is a result of the reaction between released lime and the (IGBFS), which produces more calcium silicate, aluminate, and aluminium silicate hydrates. These hydrates are embedded in the pore system and boost compressive strength.

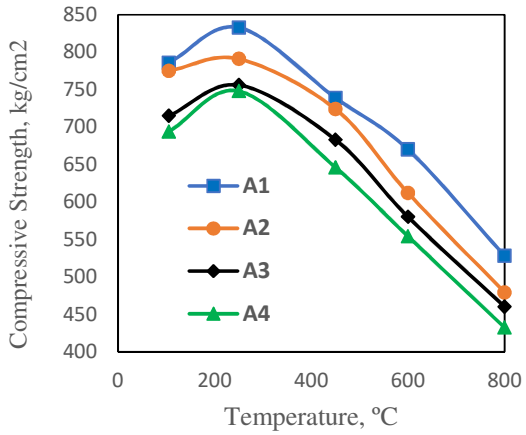

Figure (5): Mechanical strength variation for specimens treated up to 800°C

3.5. X-Ray diffraction analysis:

Crushed samples from compressive strength tests that had been dried and burned were pulverized for X-ray diffraction. The XRD patterns of 40% IGBFS (A4) cement pastes thermally treated at 250 °C and 800 °C are shown in Figure (6). The treatment temperature causes a decrease in the intensity of the (CH) characteristic lines (4.90, 2.62, 1.92, and 1.79 Aº). The lines of tobermorite and CSH are still visible at 800 °C but the lines of (CH) have almost completely vanished. When CaO reacts with SiO_2 from slag, anhydrous calcium silicate phases such β-C_2S form around 800 °C, causing new lines to appear. Alite decreases whereas belite increases. This is because the C/S ratio in pozzolanic cement has decreased. The majority of the hydrated phases vanished at 800 °C and were primarily replaced by crystalline phases with a structure resembling that of β-C_2S [35]. During diffraction lines (2.84698, 2.74999, 2.18954 and 2.03751). The breakdown of the CSH and tobermorite phases, as well as the breakdown of $Ca(OH)_2$ and $CaCO_3$, all contribute to the creation of β-C_2S. The same is true for C_2S, and this is present in every heated specimen [35]. The cement pastes demonstrate that $Ca(OH)_2$ and calcite dissolved into CaO are slightly revealed from the calcination of $CaCO_3$ to generate CaO, which can be rehydrated in the ambient air, as the heat treatment is increased beyond 500 °C.

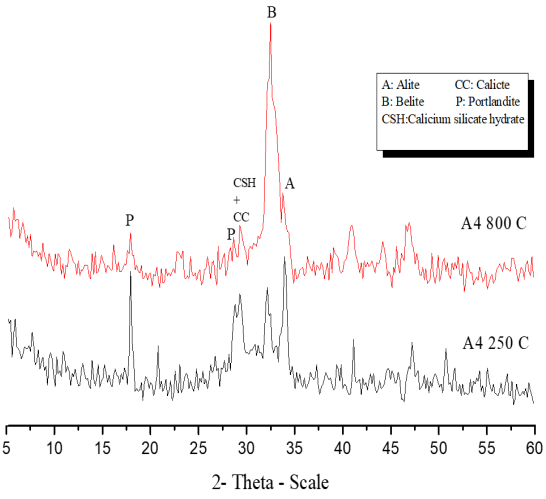

Figure (6): XRD patterns of (40 % IGBFS + 60 % OPC) specimen heated at 250 and 800 ºC

4. Conclusion

The main conclusion derived from the partial replacement of OPC by (IGBFS) may be summarized as follows:

1. Weight loss typically increases as the treatment temperature rises to 800°C.
2. In comparison to other pozzolanic cement pastes, A4 rich in OPC has a smaller porosity and a higher apparent density.
3. In comparison to other pozzolanic cement pastes, A1 rich in (IGBFS) is more heat resistant at all temperatures, has higher compressive strength, and loses less weight, making it a good choice for fire-resistance bonding materials.

5. Conflicts of interest

There are no conflicts to declare.

6. References

1. Khattab, M., Hachemi, S., Al Ajlouni, M.F.: Evaluating the physical and mechanical properties of concrete prepared with recycled refractory brick aggregates after elevated temperatures' exposure. *Constr. Build. Mater.***311**, 125351 **(2021)**.

https://doi.org/10.1016/j.conbuildmat.2021.125351
2. El Abidine Rahmouni, Z., Tebbal, N.: Mechanical Behavior of High-Performance Concrete under Thermal Effect. *Compressive Strength Concr.* 105 **(2020)**. https://doi.org/10.5772/intechopen.89916
3. Tebbal, N., Rahmouni, Z.E.A., Maza, M.: Combined effect of silica fume and additive on the behavior of high performance concretes subjected to high temperatures. *Min. Sci.***24**, 129–145 **(2017)**. https://doi.org/10.5277/msc172408
4. Sharma, A., Bošnjak, J., Bessert, S.: Experimental investigations on residual bond performance in concrete subjected to elevated temperature. *Eng. Struct.***187**, 384–395 **(2019)**. https://doi.org/10.1016/j.engstruct.2019.02.061
5. Salvia, M., Reckien, D., Pietrapertosa, F., Eckersley, P., Spyridaki, N.A., Krook-Riekkola, A., Olazabal, M., De Gregorio Hurtado, S., Simoes, S.G., Geneletti, D., Viguié, V., Fokaides, P.A., Ioannou, B.I., Flamos, A., Csete, M.S., Buzasi, A., Orru, H., de Boer, C., Foley, A., Rižnar, K., Matosović, M., Balzan, M. V., Smigaj, M., Baštáková, V., Streberova, E., Šel, N.B., Coste, L., Tardieu, L., Altenburg, C., Lorencová, E.K., Orru, K., Wejs, A., Feliu, E., Church, J.M., Grafakos, S., Vasilie, S., Paspaldzhiev, I., Heidrich, O.: Will climate mitigation ambitions lead to carbon neutrality? An analysis of the local-level plans of 327 cities in the EU. *Renew. Sustain. Energy Rev.***135**, 110253 **(2021)**. https://doi.org/10.1016/j.rser.2020.110253
6. Li, Y., Lan, S., Ryberg, M., Pérez-Ramírez, J., Wang, X.: A quantitative roadmap for China towards carbon neutrality in 2060 using methanol and ammonia as energy carriers. *iScience*. **24**, 102513 **(2021)**. https://doi.org/10.1016/j.isci.2021.102513
7. He, Z., Wang, S., Mahoutian, M., Shao, Y.: Flue gas carbonation of cement-based building products. *J. CO2 Util.***37**, 309–319 **(2020)**. https://doi.org/10.1016/j.jcou.2020.01.001
8. Yi, Z., Wang, T., Guo, R.: Sustainable building material from CO2mineralization slag: Aggregate for concretes and effect of CO2curing. *J. CO2 Util.***40**, 101196 **(2020)**. https://doi.org/10.1016/j.jcou.2020.101196
9. Xiao, J., Xiao, Y., Liu, Y., Ding, T.: Carbon emission analyses of concretes made with recycled materials considering CO2 uptake through carbonation absorption. *Struct. Concr.***22**, E58–E73 **(2021)**. https://doi.org/10.1002/suco.201900577
10. Yan, H., Zhang, J., Zhao, Y., Zheng, C.: CO2 Sequestration from flue gas by direct aqueous mineral carbonation of wollastonite. *Sci. China Technol. Sci.***56**, 2219–2227 **(2013)**
11. Koksal, F., Kocabeyoglu, E.T., Gencel, O., Benli, A.: The effects of high temperature and cooling regimes on the mechanical and durability properties of basalt fiber reinforced mortars with silica fume. *Cem. Concr. Compos.***121**, 104107 **(2021)**. https://doi.org/10.1016/j.cemconcomp.2021.104107
12. Gencel, O., Nodehi, M., Yavuz Bayraktar, O., Kaplan, G., Benli, A., Gholampour, A., Ozbakkaloglu, T.: Basalt fiber-reinforced foam concrete containing silica fume: An experimental study. *Constr. Build. Mater.***326**, 126861 **(2022)**. https://doi.org/10.1016/j.conbuildmat.2022.126861
13. Rehsi, S.S., Garg, S.K.: Heat resistance of Portland fly ash cement. **(2012)**
14. Morsy, M.S., Shebl, S.S.: Effect of silica fume and metakaoline pozzolana on the performance of blended cement pastes against fire. *Ceram. - Silikaty*. **51**, 40–44 **(2007)**
15. El-Didamony, H., Khalil, K.A.: Physicochemical and fire resistance characteristics of artificial pozzolanic cement pastes. *Egypt. J. Chem.***56**, 155–168 **(2013)**. https://doi.org/10.21608/ejchem.2013.1105
16. Li, Y., Luo, Y., Du, H., Liu, W., Tang, L., Xing, F.: Evolution of Microstructural Characteristics of Carbonated Cement Pastes Subjected to High Temperatures Evaluated by MIP and SEM. *Materials (Basel).***15**, 6037 **(2022)**. https://doi.org/10.3390/ma15176037
17. Nhau, N. cứu thực nghiệm ảnh hưởng của tro trấu tới cường độ của vữa ở các nhiệt độ khác: Experimental study on influence of rice husk ash on mortar compressive strength at different temperatures. *DTU J. Sci. Technol.***3**, 51–59 **(2022)**
18. El-Didamony, H., Heikal, M., Moselhy, H., Ali, M.A.: Utilization of GBFS in the preparation of low cost cement. *Egypt. J. Chem.***59**, 623–636 **(2016)**. https://doi.org/10.21608/ejchem.2016.1439
19. Aydın, S., Baradan, B.: Effect of activator type and content on properties of alkali-activated slag mortars. *Compos. Part B Eng.***57**, 166–172 **(2014)**
20. Sharma, A.K., Sivapullaiah, P. V.: Ground granulated blast furnace slag amended fly ash as an expansive soil stabilizer. *Soils Found.***56**, 205–212 **(2016)**. https://doi.org/10.1016/j.sandf.2016.02.004

21. Wang, X.-Y., Lee, H.-S.: Modeling the hydration of concrete incorporating fly ash or slag. *Cem. Concr. Res.***40**, 984–996 **(2010)**
22. ASTM C204: Standard Test Methods for Fineness of Hydraulic Cement by Air-Permeability. *ASTM Int. West Conshohocken, PA*. 1–10 **(2011)**
23. Heikal, M., Al-Duaij, O.K., Ibrahim, N.S.: Microstructure of composite cements containing blast-furnace slag and silica nano-particles subjected to elevated thermally treatment temperature. *Constr. Build. Mater.***93**, 1067–1077 **(2015)**. https://doi.org/10.1016/j.conbuildmat.2015.05.042
24. Heikal, M., Nassar, M.Y., El-Sayed, G., Ibrahim, S.M.: Physico-chemical, mechanical, microstructure and durability characteristics of alkali activated Egyptian slag. *Constr. Build. Mater.***69**, 60–72 **(2014)**
25. Designation, A.: C191: Standard test method for normal consistency and setting time of Hydraulic Cement ". *Annu. B. ASTM Stand.* 172–174 **(2008)**
26. Heikal, M.: Effect of temperature on the structure and strength properties of cement pastes containing fly ash alone or in combination with limestone. *Ceram. - Silikaty*. **50**, 167–177 **(2006)**
27. Heikal, M., Abd El Aleem, S., Morsi, W.M.: Characteristics of blended cements containing nano-silica. *HBRC J.***9**, 243–255 **(2013)**. https://doi.org/10.1016/j.hbrcj.2013.09.001
28. Yazıcı, Ş., Sezer, G.İ., Şengül, H.: The effect of high temperature on the compressive strength of mortars. *Constr. Build. Mater.***35**, 97–100 **(2012)**. https://doi.org/https://doi.org/10.1016/j.conbuildmat.2012.02.082
29. Lin, R.S., Han, Y., Wang, X.Y.: Macro–meso–micro experimental studies of calcined clay limestone cement (LC3) paste subjected to elevated temperature. *Cem. Concr. Compos.***116**, 103871 **(2021)**. https://doi.org/10.1016/j.cemconcomp.2020.103871
30. Beuvier, T., Bardeau, J.F., Calvignac, B., Corbel, G., Hindré, F., Grenèche, J.M., Boury, F., Gibaud, A.: Phase transformations in CaCO3/iron oxide composite induced by thermal treatment and laser irradiation. *J. Raman Spectrosc.***44**, 489–495 **(2013)**. https://doi.org/10.1002/jrs.4200
31. ASTM C109/C109M-02: Standard Test Method for Compressive Strength of Hydraulic Cement Mortars. ASTM International (2020)
32. Heikal, M., Aiad, I.: Influence of delaying addition time of superplasticizers on chemical process and properties of cement pastes. *Ceram. - Silikaty*. **52**, 8–15 **(2008)**
33. El-Didamony, H., El-Rahman, E.A., Osman, R.M.: Fire resistance of fired clay bricks-fly ash composite cement pastes. *Ceram. Int.***38**, 201–209 **(2012)**. https://doi.org/10.1016/j.ceramint.2011.06.050
34. Khan, M., Cao, M., Chaopeng, X., Ali, M.: Experimental and analytical study of hybrid fiber reinforced concrete prepared with basalt fiber under high temperature. *Fire Mater.***46**, 205–226 **(2022)**. https://doi.org/10.1002/fam.2968
35. Wang, D., Noguchi, T., Nozaki, T., Higo, Y.: Investigation on the fast carbon dioxide sequestration speed of cement-based materials at 300 °C–700 °C. *Constr. Build. Mater.***291**, 123392 **(2021)**. https://doi.org/10.1016/j.conbuildmat.2021.123392